



HAL
open science

H_∞ observer design for singular nonlinear parameter-varying system

Manh-Hung Do, Damien Koenig, Didier Theilliol

► **To cite this version:**

Manh-Hung Do, Damien Koenig, Didier Theilliol. H_∞ observer design for singular nonlinear parameter-varying system. CDC 2020 - 59th IEEE Conference on Decision and Control, Dec 2020, Jeju Island, South Korea. 10.1109/CDC42340.2020.9303844 . hal-02793187

HAL Id: hal-02793187

<https://hal.science/hal-02793187>

Submitted on 5 Jun 2020

HAL is a multi-disciplinary open access archive for the deposit and dissemination of scientific research documents, whether they are published or not. The documents may come from teaching and research institutions in France or abroad, or from public or private research centers.

L'archive ouverte pluridisciplinaire **HAL**, est destinée au dépôt et à la diffusion de documents scientifiques de niveau recherche, publiés ou non, émanant des établissements d'enseignement et de recherche français ou étrangers, des laboratoires publics ou privés.

\mathcal{H}_∞ observer design for Singular Nonlinear Parameter-varying System

Manh-Hung Do, Damien Koenig, and Didier Theilliol

Abstract—The main contribution of this paper is an \mathcal{H}_∞ observer design for a class of singular Nonlinear Parameter-varying system in the presence of disturbances and Lipschitz nonlinearity. In specific, this observer tackles the impact of disturbance on estimation error thanks to the \mathcal{H}_∞ norm, while the parameter-dependent stability of estimation dynamics helps to widen the feasible region of LMI solution under the Lipschitz constraint. Finally, a numerical example with the gridding solution is illustrated to highlight the proposed design.

Index Terms—Nonlinear Parameter-varying system, Lipschitz condition, Linear parameter-varying system (LPV), Observer design, singular (descriptor) system.

I. INTRODUCTION

Over the last few years, the linear parameter-varying (LPV) modeling methodology has been widely implemented in many vehicle and aerospace control analyses [1]. In which, the non-linear systems are displayed in the linear system representation where the distribution matrices depend on measurable/estimated time-varying parameters (TVP). Therefore, the LPV modeling allows system behavior to adapt to different working points. Later, the original LPV systems have been extended to the singular LPV system (S-LPV) by taking into account the static constraints, which facilitates the modeling of a variety of engineering systems such as chemical, mineral and economic processes [2]. Thanks to the great number of works in the singular system, many studies have developed the implementation of S-LPV estimator-observer design in state-fault estimation. To handle the disturbance impact and fault estimation problem, authors in [3] have developed an unknown input proportional-integral observer. However, its restrictive disturbance-decoupling condition cannot be always satisfied, which leads to the application of \mathcal{H}_∞ (induced \mathcal{L}_2) norm to disturbance attenuation. In [4], the \mathcal{H}_∞ proportional-derivative observer, whose singular representation is a challenge for practical implementation, has been introduced. In [5], a fast adaptive estimation observer is proposed to estimate the faults with bounded derivatives in the S-LPV system. Meanwhile, for the S-LPV system whose TVP cannot be directly measured but possibly estimated, the \mathcal{H}_∞ functional observer is presented in the work of Lopez-Estrada et al. [6] to attenuate the impact of TVP uncertainty on state estimation. Despite the effective

performance of the above designs, the requirement of LPV polytopic representation limits their implementation.

On the other hand, as the time-varying parameters are displayed in nonlinear form in many applications, the nonlinear behavior of the original system cannot be expressed correctly. As a result, there has been an appealing interest in the research community for nonlinear parameter varying (NLPV) systems, which integrate the non-linear parts into the usual LPV system with linear-parameter dependence. In [7], a polytopic observer has been introduced for the NLPV model of diesel engines with once-differentiable nonlinearity. Authors in [8] also developed an \mathcal{H}_∞ output-feedback controller for NLPV model, but its constraints in LMI optimization to handle Lipschitz condition can lead to an unfeasible solution. Recently, this issue has been relaxed in the study on the stability of the NLPV closed-loop system by using a state-feedback controller [9] with parameter-dependent Lipschitz dynamics. In [10], the \mathcal{H}_∞ polytopic Luenberger observer has also been considered for the NLPV model of the suspension system to estimate nonlinear damper force under the influence of road disturbance. However, all the above studies for NLPV only promote the parameter-independent stability which narrows the feasible solution region in certain circumstances.

The lack of study for parameter-dependent stability against this nonlinear phenomenon and the idea of a wider class than S-LPV system have motivated the following contributions in this paper for the LPV framework:

- A new class of singular NLPV system considering Lipschitz nonlinearity (S-NLPV) is introduced, which unifies all the so far existing kinds of LPV systems;
- An \mathcal{H}_∞ observer design-based process for the S-NLPV system is studied. In which, both disturbance attenuation and parameter-dependent stability are ensured thanks to LMI optimization under the Lipschitz constraint.

A numerical example will be illustrated to prove the performance of observer design in the S-NLPV system.

The paper is organized as follows. Firstly, the problem formulation of the S-NLPV system is presented in Section 2. Then, Section 3 demonstrates in detail the methodology of the observer design to attenuate disturbance on estimation results. The grid-based LMI solution and the existence conditions for the observer are discussed in Section 4. Later, Section 5 illustrates a numerical example with the corresponding frequency analysis. Finally, the conclusion with future work is presented in Section 6.

Notations: \mathbb{R}^n and $\mathbb{R}^{m \times n}$ respectively represent the n -dimensional Euclidean space and the set of all $m \times n$ real

This work is supported by the ITEA3 European Project through EMPHYSIS under Grant 15016.

Manh-Hung Do and Damien Koenig are with Univ. Grenoble Alpes, CNRS, Grenoble INP, GIPSA-lab, 38000 Grenoble, France. manh-hung.do@gipsa-lab.grenoble-inp.fr; damien.koenig@gipsa-lab.grenoble-inp.fr

Didier Theilliol is with University of Lorraine, CRAN, UMR 7039, Campus Sciences, B.P.70239, 54506 Vandoeuvre-les-Nancy Cedex, France. didier.theilliol@univ-lorraine.fr

matrices; X^T is the transpose of the matrix X ; 0 and I denote respectively the zero and the identity matrix with appropriate dimensions; the symbol $(*)$ denotes the transposed block in the symmetric position; X^\dagger is the Moore-Penrose inverse of X ; the term $i = 1 : N$ means $i \in \{1, 2, \dots, N-1, N\}$; $\Re(x)$ is the real part of the complex number x ; and we denote $\mathcal{H}\{A\} = A + A^T$.

II. PROBLEM FORMULATION

Consider the following class of singular NLPV:

$$\begin{cases} E\dot{x} &= A_{(\rho)}x + B_{(\rho)}u + B_{\phi(\rho)}\phi(x, u) + D_{1(\rho)}w \\ y &= C_yx + D_2w \\ z &= C_zx \end{cases} \quad (1)$$

In which,

- $x \in \mathbb{R}^{n_x}$ is the state vector; $y \in \mathbb{R}^{n_y}$ is the measurement output vector; $u \in \mathbb{R}^{n_u}$ is the input vector; $w \in \mathbb{R}^{n_d}$ is the disturbance vector with bounded energy; and $z \in \mathbb{R}^{n_z}$ is the vector of the desired signals, which can be state x or a combination of x , to be estimated.
- Time-varying measurable parameter ρ takes values in the parameter space \mathcal{P}_ρ :

$$\mathcal{P}_\rho = \{\rho = [\rho_1(t) \ \rho_2(t) \ \dots \ \rho_p(t)]^T \mid \underline{\rho}_i \leq \rho_i(t) \leq \bar{\rho}_i, \forall i = 1 : p, t \geq 0. \quad (2)$$

The following assumptions are considered in this paper:

- (A.1) Parameter variations are bounded. In other words, $|\dot{\rho}_i| \leq \vartheta_i$ where ϑ_i is non-negative constant boundness [11].
- (A.2) Nonlinear term $\phi(x, u)$ with bounded u (due to saturation in practice) is a Lipschitz function that satisfies:

$$\|\tilde{\phi}\| = \|\phi(x, u) - \phi(\hat{x}, u)\| \leq \gamma \|x - \hat{x}\| \quad (3)$$

for all $x, \hat{x} \in \mathbb{R}^{n_x}$, where γ is known Lipschitz constant.

In the observer design, \hat{x} is the estimated of the state x .

- (A.3) S-NLPV system (1) is impulse-free and R-detectable $\forall \rho$, which is later analytically verified by the conditions discussed in Section 4.B.

Under the assumptions (A.1)-(A.3), the aim of this paper is to determine a NLPV observer that has the form:

$$\begin{cases} \dot{\xi} &= F_{(\rho)}\xi + J_{(\rho)}u + L_{(\rho)}y + TB_{\phi(\rho)}\phi(\hat{x}, u) \\ \dot{\hat{x}} &= \xi + Ny \\ \dot{\hat{z}} &= C_z\hat{x} \end{cases}, \quad (4)$$

such that the following objectives are satisfied:

- (O.1) When $w^* = [w^T \ \dot{w}^T]^T = 0$, the dynamics of estimation errors, which is then illustrated in (15), is asymptotically stable.
- (O.2) When $w^* \neq 0$, the impact of disturbance w^* on the desired estimation error $e_z = z - \hat{z}$ is attenuated, i.e.

$$\sup_{\rho \in \mathcal{P}_\rho} \sup_{\|w^*\|_2 \neq 0, w^* \in \mathcal{L}_2} \frac{\|e_z\|_2}{\|w^*\|_2} \leq \gamma_\infty. \quad (5)$$

where ξ is the observer state; \hat{z} is the estimated of z , which is useful to design the state-feedback controller ($C_z = I_{n_z}$), as well as the output-feedback controller ($C_z \neq I_{n_z}$); the observer

matrices $F_{(\rho)}$, $J_{(\rho)}$, T , $L_{(\rho)}$, and N are later synthesized in Section 3.

Remark 1: If the system output y depends on the time-varying parameter ρ , i.e. $y = C_{y(\rho)}x + D_{2(\rho)}w$, the structure of system (1) can always be obtained. More details are discussed in Appendix.

In the next section, design process for the \mathcal{H}_∞ -based observer for the S-NPLV system (1) is presented.

III. FULL-ORDER NLPV OBSERVER DESIGN

The state estimation error $e = x - \hat{x}$ can be expressed as:

$$e = x - \hat{x} = x - (\xi + Ny) \quad (6)$$

$$= (I - NC_y)x - \xi - ND_2w, \quad (7)$$

$$= TE x - \xi - ND_2w, \quad (8)$$

where the matrix T has to ensure the constraint:

$$TE + NC_y = I. \quad (9)$$

Hence, from (1), (4) and (8), the error dynamics is demonstrated as:

$$\dot{e} = TE\dot{x} - \dot{\xi} - ND_2\dot{w} \quad (10)$$

$$\begin{aligned} &= F_{(\rho)}e + TB_{\phi(\rho)}\tilde{\phi} + (J_{(\rho)} - TB_{(\rho)})u \\ &\quad + (TA_{(\rho)} - F_{(\rho)}TE - L_{(\rho)}C_y)x - ND_2\dot{w} \\ &\quad + [TD_{1(\rho)} + (F_{(\rho)}N - L_{(\rho)})D_2]w. \end{aligned} \quad (11)$$

Then, by choosing the following conditions:

$$J_{(\rho)} - TB_{(\rho)} = 0, \quad (12)$$

$$TA_{(\rho)} - F_{(\rho)}TE - L_{(\rho)}C_y = 0, \quad (13)$$

$$K_{(\rho)} = -F_{(\rho)}N + L_{(\rho)}, \quad (14)$$

the dynamics (11) is rewritten as:

$$\dot{e} = F_{(\rho)}e + TB_{\phi(\rho)}\tilde{\phi} + [(TD_{1(\rho)} - K_{(\rho)}D_2) \quad -ND_2]w^*. \quad (15)$$

From Eqs. (9), (13) and (14), it follows that:

$$TA_{(\rho)} - K_{(\rho)}C_y - F_{(\rho)} = 0. \quad (16)$$

From condition (9), we obtain:

$$\begin{bmatrix} T & N \end{bmatrix} \begin{bmatrix} E \\ C_y \end{bmatrix} = I. \quad (17)$$

If $\text{rank} \begin{bmatrix} E \\ C_y \end{bmatrix} = n_x$, which is also the impulse-free condition, it follows that:

$$\begin{bmatrix} T & N \end{bmatrix} = \begin{bmatrix} E \\ C_y \end{bmatrix}^\dagger. \quad (18)$$

Also, it is noted that $\begin{bmatrix} T & N \end{bmatrix}$ is a full-row rank matrix.

Thus, the matrices T and N can be calculated by:

$$T = \begin{bmatrix} E \\ C_y \end{bmatrix}^\dagger \delta_T, \quad N = \begin{bmatrix} E \\ C_y \end{bmatrix}^\dagger \delta_N, \quad (19)$$

where: $\delta_T = \begin{bmatrix} I \\ 0 \end{bmatrix}$ and $\delta_N = \begin{bmatrix} 0 \\ I \end{bmatrix}$.

Eq. (15) yields that:

$$\begin{cases} \dot{e} &= F_{(\rho)}e + B_{e(\rho)}\tilde{\phi} + W_{(\rho)}w^*, \\ e_z &= C_z e \end{cases} \quad (20)$$

where

$$e_z = z - \hat{z} = C_z(x - \hat{x}) = C_z e, \quad (21)$$

$$F_{(\rho)} = TA_{(\rho)} - K_{(\rho)}C_y, \quad (22)$$

$$B_{e(\rho)} = TB_{\phi(\rho)}, \quad (23)$$

$$W_{(\rho)} = [W_{1(\rho)} \quad W_{2(\rho)}], \quad (24)$$

$$W_{1(\rho)} = TD_{1(\rho)} - K_{(\rho)}D_2, \quad (25)$$

$$W_{2(\rho)} = -ND_2, \quad (26)$$

and the gain $K_{(\rho)}$ is derived from the following Theorem, which satisfies the objectives (O.1)-(O.2).

Theorem 1: Under the assumptions (A.1)-(A.3), the design objectives (O.1)-(O.2) are achieved if there exist symmetric positive definite matrices $P_{(\rho)}$ and matrix $Y_{(\rho)}$, positive scalar ε which minimize γ_∞ and satisfy that:

$$\begin{bmatrix} \Omega_{11(\rho)} + \eta & \Omega_{12(\rho)} & \Omega_{13(\rho)} & \Omega_{14(\rho)} & C_z^T \\ (*) & -\varepsilon I & 0 & 0 & 0 \\ (*) & (*) & -\gamma_\infty I & 0 & 0 \\ (*) & (*) & (*) & -\gamma_\infty I & 0 \\ (*) & (*) & (*) & (*) & -I \end{bmatrix} < 0, \quad (27)$$

where

$$\Omega_{11(\rho)} = \sum_i^p \pm \vartheta_i \frac{\partial P_{(\rho)}}{\partial \rho_i} + \mathcal{H}\{P_{(\rho)}TA_{(\rho)} + Y_{(\rho)}C_y\}, \quad (28)$$

$$\Omega_{12(\rho)} = P_{(\rho)}TB_{\phi(\rho)}, \quad (29)$$

$$\Omega_{13(\rho)} = P_{(\rho)}TD_{1(\rho)} + Y_{(\rho)}D_2, \quad (30)$$

$$\Omega_{14(\rho)} = -P_{(\rho)}ND_2, \quad (31)$$

$$\eta = \varepsilon(\gamma I)^T(\gamma I), \quad (32)$$

then the matrix $K_{(\rho)}$ is calculated by: $K_{(\rho)} = -P_{(\rho)}^{-1}Y_{(\rho)}$.

Using matrices T and N , (22) yields the matrix $F_{(\rho)}$, while the matrices $J_{(\rho)}$ and $L_{(\rho)}$ are calculated from (12) and (14).

Remark 2: The notion $\sum_i^p \pm(\cdot)$ expresses all combinations of $+(\cdot)$ and $-(\cdot)$ that are included in the inequality (27). Consequently, the inequality (27) actually represents 2^p different inequalities that correspond to the 2^p different combinations in the summation.

Proof: Choose the parameter-dependent LPV Lyapunov function [12]:

$$V_{(\rho)} = e^T P_{(\rho)} e, \quad (33)$$

with $P_{(\rho)} > 0$.

Combined with the above Lyapunov function, the sufficient condition for disturbance attenuation (5) can be rewritten as [11]:

$$J_\infty = \dot{V}_{(\rho)} + e_z^T e_z - \gamma_\infty w^{*T} w^* < 0. \quad (34)$$

Also, the Lipschitz condition (3) yields the constraint:

$$\|\tilde{\phi}\| \leq \gamma \|e\| \Rightarrow J = (\tilde{\phi})^T (\tilde{\phi}) - e^T (\gamma I)^T (\gamma I) e \leq 0, \quad (35)$$

By applying the S-procedure [13], the two above constraints in Eqs. (34)-(35) can be satisfied if there exists a positive scalar ε such that:

$$J_\infty - \varepsilon J < 0 \quad (36)$$

From LPV Lyapunov function, it follows that:

$$\begin{aligned} \dot{V}_{(\rho)} &= e^T \frac{\partial P_{(\rho)}}{\partial t} e + \mathcal{H}\{e^T P_{(\rho)} \dot{e}\}, \\ &= e^T \frac{\partial P_{(\rho)}}{\partial t} e + \mathcal{H}\{e^T P_{(\rho)} F_{(\rho)} e + e^T P_{(\rho)} B_{e(\rho)} \tilde{\phi} \\ &\quad + e^T P_{(\rho)} W_{(\rho)} w^*\} \end{aligned} \quad (37)$$

Using Eq. (20), we obtain:

$$\begin{aligned} \dot{V}_{(\rho)} &\leq \Upsilon^T \begin{bmatrix} \Omega_{11(\rho)} & \Omega_{12(\rho)} & [\Omega_{13(\rho)} & \Omega_{14(\rho)}] \\ (*) & (*) & 0 \\ (*) & (*) & 0 \end{bmatrix} \Upsilon \\ &= \Upsilon^T \Omega_{(\rho)} \Upsilon, \end{aligned} \quad (39)$$

where $\Upsilon = [e^T \quad \tilde{\phi}^T \quad w^{*T}]^T$.

The constraint (36) is guaranteed if:

$$\Upsilon^T \Omega_{(\rho)} \Upsilon + e_z^T e_z - \gamma_\infty w^{*T} w^* - \varepsilon J < 0, \quad (40)$$

$$\begin{aligned} \Upsilon^T \Omega_{(\rho)} \Upsilon + e^T C_z^T C_z e - \gamma_\infty w^{*T} w^* - \varepsilon (\tilde{\phi})^T (\tilde{\phi}) \\ + \varepsilon e^T (\gamma I)^T (\gamma I) e < 0, \end{aligned} \quad (41)$$

which is equivalent to the following LMI $\forall \Upsilon \neq 0$:

$$\begin{bmatrix} \Omega'_{11(\rho)} + C_z^T C_z + \eta & \Omega_{12(\rho)} & \Omega_{13(\rho)} & \Omega_{14(\rho)} \\ (*) & -\varepsilon I & 0 & 0 \\ (*) & (*) & -\gamma_\infty I & 0 \\ (*) & (*) & (*) & -\gamma_\infty I \end{bmatrix} < 0, \quad (42)$$

where

$$\Omega'_{11(\rho)} = \dot{P} \frac{\partial P_{(\rho)}}{\partial \rho} + \mathcal{H}\{P_{(\rho)}TA_{(\rho)} + Y_{(\rho)}C_y\}. \quad (43)$$

To avoid the direct handling of derivative \dot{P} , as mentioned in [11], the inequality (42) only holds if the following simplified condition is verified.

$$\begin{bmatrix} \Omega_{11(\rho)} + C_z^T C_z + \eta & \Omega_{12(\rho)} & \Omega_{13(\rho)} & \Omega_{14(\rho)} \\ (*) & -\varepsilon I & 0 & 0 \\ (*) & (*) & -\gamma_\infty I & 0 \\ (*) & (*) & (*) & -\gamma_\infty I \end{bmatrix} < 0. \quad (44)$$

By applying the Schur complement [13] to above inequality, the condition (27) is obtained, which completes the proof. \blacksquare

IV. GENERAL DISCUSSION

A. Gridding-based approach of LMI solution

In the Theorem 1, since the matrices $P_{(\rho)}$ and $Y_{(\rho)}$ depend on the values of parameter-varying vector ρ , the LMI (27) requires an effective solution in order to satisfy all conditions and deal with the coupling of parameter-varying matrices $P_{(\rho)}$ and $Y_{(\rho)}$. Therefore, as already discussed in [14], the gridding-based approach is proposed. More details about the standard gridding solution, particularly its effectiveness, are

given in [14]–[16]. In this approach, there are two aspects to be considered:

1. Choice of basis functions $P_{(\rho)}$ and $Y_{(\rho)}$

By approximating the matrices $P_{(\rho)}$ and $Y_{(\rho)}$ with finite basis functions of ρ , a solution for the LMI (27) can be achieved through an infinite dimensional set. Unfortunately, to the best of authors' knowledge, the choice depends heavily on practice. Regarding simplicity, polynomials are used, which facilitates the formulations of $\partial P_{(\rho)}/\partial \rho$. For example, $P_{(\rho)} = P_0 + \rho P_1$, where the parameter matrices P_0 and P_1 are constant matrices satisfying that $P_{(\rho)} > 0$. More details on practical choices are presented in [15]–[17], while the LMI optimization problem is solved through the implementation of [18], [19].

2. The number of gridding points $n_g^{\rho_i}$ (the number of gridding points for element ρ_i of vector ρ)

The number of gridding points decides the gridding space for LMI computation and its complexity. However, to the best of authors' knowledge, there has not been any exact method to choose $n_g^{\rho_i}$. Overall, the appropriate number $n_g^{\rho_i}$ of points must be neither too small to assure the performance and stability of the observer-controller design, nor too large to avoid the numerical problem and computation complexity. Also, the distance between each point in the grid should be considered as it may cause disturbances in the transition of each subsystem.

B. Existence of observer design

In the gridding-based approach, the (singular) LPV system (under Lipschitz condition) is considered as (singular) linear time-invariant (LTI) system at each time-frozen gridding point ρ^j ($j = 1 : N$, $N = n_g^{\rho_1} \times n_g^{\rho_2} \times \dots \times n_g^{\rho_p}$) [12]. Therefore, the existence conditions for the observer design can be analytically derived for each point ρ^j in the grid as follows.

B.1. Condition for the solution of (19)

As mentioned in (17), the requirement for the existence of T and N is the impulse-free condition, which is independent of time-varying parameter ρ :

$$(C.1) \quad \text{rank} \begin{bmatrix} E \\ C_y \end{bmatrix} = n_x. \quad (45)$$

B.2. Stability condition of error dynamics in (20)

The feasibility of Theorem 1 implies that $F_{(\rho^j)}$ is Hurwitz for each time-frozen ρ^j . In other words, there exists a matrix gain $\tilde{Z}_{(\rho^j)}$ such that $F_{(\rho^j)}$ is stable if and only if the pair $(TA_{(\rho^j)}, C_y)$ is R-detectable. That is explained by the relation in (22) that:

$$F_{(\rho^j)} = TA_{(\rho^j)} - K_{(\rho^j)}C_y. \quad (46)$$

This R-detectability condition is equivalent to:

$$(C.2) \quad \text{rank} \begin{bmatrix} sE - A_{(\rho^j)} \\ C_y \end{bmatrix} = n_x, \forall j = 1 : N, \mathcal{R}(s) \geq 0. \quad (47)$$

Proof: The condition (C.2) is equivalent to:

$$\text{rank} \begin{bmatrix} sE - A_{(\rho^j)} \\ C_y \end{bmatrix} = n_x, \forall j = 1 : N, \mathcal{R}(s) \geq 0. \quad (48)$$

$$\Leftrightarrow \text{rank} \begin{bmatrix} sE - A_{(\rho^j)} \\ sC_y \\ C_y \end{bmatrix} = n_x, \forall j = 1 : N, \mathcal{R}(s) \geq 0. \quad (49)$$

By defining the matrix $X = \begin{bmatrix} T & N & 0 \\ 0 & I_{n_y} & -sI_{n_y} \\ 0 & 0 & I_{n_y} \end{bmatrix}$, the above condition is equivalent to:

$$\text{rank}(X \begin{bmatrix} sE - A_{(\rho^j)} \\ sC_y \\ C_y \end{bmatrix}) = n_x, \forall j = 1 : N, \mathcal{R}(s) \geq 0. \quad (50)$$

$$\Leftrightarrow \text{rank} \begin{bmatrix} sTE - TA_{(\rho^j)} + sNC_y \\ 0 \\ C_y \end{bmatrix} = n_x, \quad \forall j = 1 : N, \mathcal{R}(s) \geq 0. \quad (51)$$

As $TE + NC_y = I$, it follows that:

$$\text{rank} \begin{bmatrix} sI - TA_{(\rho^j)} \\ C_y \end{bmatrix} = n_x, \forall j = 1 : N, \mathcal{R}(s) \geq 0. \quad (52)$$

That is also the condition for R-detectability of the pair $(TA_{(\rho^j)}, C_y)$, which completes the proof. ■

As mentioned in [2], [20], a singular system can be decomposed into slow and fast subsystems. Regarding the results of the singular NLPV system, the condition (C.1) (impulse-free) presents the observability for the fast dynamics, while the condition (C.2) (R-detectability) for each frozen point ρ^j corresponds to the detectability of the slow component.

It should be noted that the condition (C.2) is only an analytically necessary condition implied for the R-detectability of S-NLPV system at each time-frozen point ρ^j in the context of the grid-based approach. In addition, the great amount N of gridding points ρ^j ($j = 1 : N$) can present/cover all behaviors of ρ in R-detectability; however, it also increases the computation cost for later LMI optimization.

V. NUMERICAL EXAMPLE

A. Model Parameters

Consider the system:

$$\begin{cases} E\dot{x} &= A_{(\rho)}x + Bu + B_\phi \sin(Kx)u + D_1w \\ y &= C_yx + D_2w \\ z &= C_zx \end{cases}, \quad (53)$$

- Desired signal $z = [z_1^T \ z_2^T]^T$ is the output to be estimated by the \mathcal{H}_∞ observer (4).
- Varying-parameter ρ is defined as: $\rho = 0.25\sin(8t) + 0.75$, so $0.5 \leq \rho \leq 1$ and $|\dot{\rho}| \leq \vartheta = 2$.
- System parameters, which satisfy the conditions (C.1) and (C.2), are chosen as following:

$$E = \begin{bmatrix} 1 & 0 & 0 \\ 0 & 1 & 0 \\ 0 & 0 & 0 \end{bmatrix}, A_{(\rho)} = \begin{bmatrix} -5 + \rho & 1 & 1 \\ 0 & -5 & 0 \\ 0.5 & 0 & -1 \end{bmatrix},$$

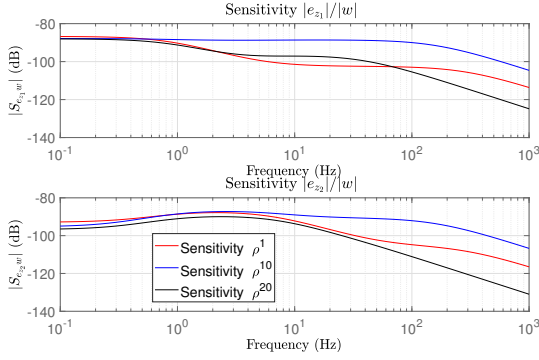


Fig. 1. Sensitivity function $|S_{e_z w}| = |e_z/w|$

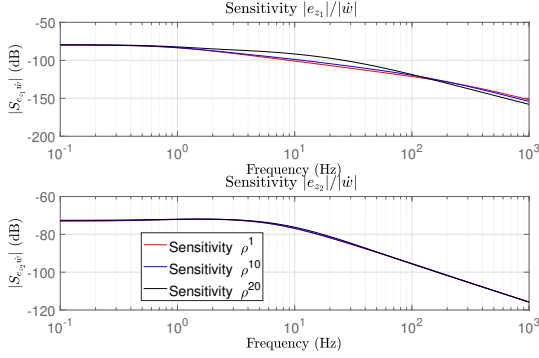


Fig. 2. Sensitivity function $|S_{e_z \dot{w}}| = |e_z/\dot{w}|$

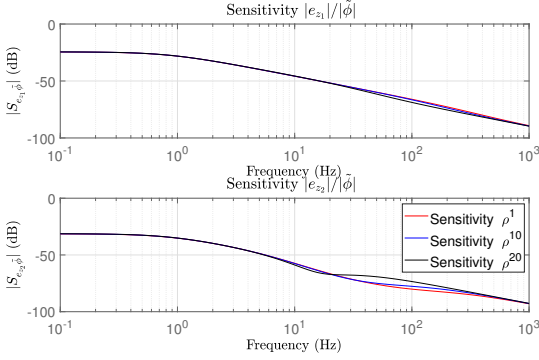


Fig. 3. Sensitivity function $|S_{e_z \tilde{\phi}}| = |e_z/\tilde{\phi}|$

$$B = \begin{bmatrix} 0 \\ 0.2 \\ 0.5 \end{bmatrix}, B_\phi = \begin{bmatrix} 0 \\ 0.2 \\ 0 \end{bmatrix}, C_y = \begin{bmatrix} 1 & 1 & -0.05 \\ 0 & 2 & -1 \end{bmatrix},$$

$$D_1 = \begin{bmatrix} 0.5 \\ 0.1 \\ 0 \end{bmatrix}, D_2 = \begin{bmatrix} 0 \\ 0.01 \end{bmatrix}, C_z = \begin{bmatrix} 1 & -1 & 0 \\ 0 & 1 & -1 \end{bmatrix},$$

and $K = \begin{bmatrix} 0 & 0 & 1 \end{bmatrix}$.

- Control input u is bounded in the region $|u| \leq u_0 = 5$, which leads to the Lipschitz condition:
$$\|\phi(x, u) - \phi(\hat{x}, u)\| \leq u_0 K \|x - \hat{x}\|, \quad (54)$$
where $\phi(x, u) = \sin(Kx)u$ and $\gamma = u_0 K$.

Thanks to the usage of Yalmip toolbox [18], sdpt3 solver [19] and grid-based methodology with $n_g = 30$ points and 2^{nd} -order basic function for $Y_{2(\rho)}$ [17], i.e.

$$P(\rho) = P_0 + \rho P_1 + \rho^2 P_2, \quad (55)$$

$$Y(\rho) = Y_0 + \rho Y_1 + \rho^2 Y_2, \quad (56)$$

then Theorem 1 is solved by finding constant matrices P_k and Y_k ($k = 0 : 2$) such that $P(\rho) > 0$ and LMI (27) are satisfied. Also, the \mathcal{H}_∞ optimal value is found as $\gamma_\infty = 0.0227$ (or -32.8795 dB) and $\varepsilon = 20.8801$.

B. Frequency Analysis

The sensitivity ρ^j in the following figures represents the frequency response at each time-frozen value ρ^j ($j = 1 : 30$) of varying parameter ρ . From (20), the sensitivity function can be analytically rewritten as:

$$S_{e_z w(\rho^j)} = C_z(pI - F(\rho^j))^{-1} W_1(\rho^j), \quad (57)$$

$$S_{e_z \dot{w}(\rho^j)} = C_z(pI - F(\rho^j))^{-1} W_2(\rho^j), \quad (58)$$

$$S_{e_z \tilde{\phi}(\rho^j)} = C_z(pI - F(\rho^j))^{-1} B_{e(\rho^j)}. \quad (59)$$

Without loss of generality, only the sensibilities ρ^1 , ρ^{10} , and ρ^{20} are presented to evaluate the whole varying range. As observed from Figs. 1-2, all sensibilities satisfy the disturbance-attenuating condition (5) with great magnitudes of attenuation less than -70 dB ($< \gamma_\infty$). Meanwhile, Fig. 3 shows an important impact of nonlinearity term $\tilde{\phi}$ (peak around -25 dB) generated by the Lipschitz condition in the low frequency domain (< 1 Hz). However, the higher the frequency, the smaller the impact of the $\tilde{\phi}$ on estimation error e_z .

C. Time-domain simulation

Simulation is realized in 3 seconds with the conditions:

- Disturbance vector is defined as: $w = \sin(4\pi t)$
- Control input: $u = u_0 \sin(8\pi t)$.
- Initial condition: $x_1(0) = 0$, $x_2(0) = 0$ and $\hat{x}_0 = [0.005 \ 0 \ 0.02]^T$.

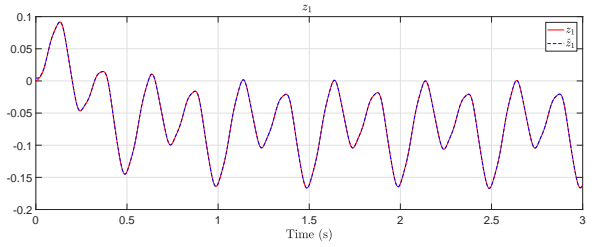


Fig. 4. z_1 estimation

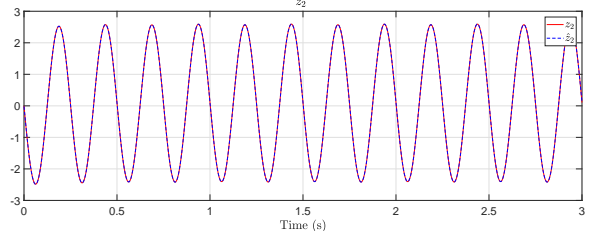


Fig. 5. z_2 estimation

TABLE I
EVALUATION FOR ESTIMATION ERROR

Signal	e_{z_1}	e_{z_2}
RMS (Root-mean-square)	0.0007	0.0025

Figs. 4-5 show that the estimated signal $\hat{z} = [\hat{z}_1^T \ \hat{z}_2^T]^T$ has successfully converged to the desired signal z with acceptable values of estimation error as illustrated in Table I. In addition, these results prove that the impact of disturbance on estimation error e is greatly attenuated while $e_z \rightarrow 0$ is ensured and the Lipschitz condition is bounded, as mentioned in frequency analysis.

VI. CONCLUSION

In this paper, a new class of singular NLPV system with Lipschitz nonlinearity is introduced, which promotes the implementation of the LPV framework in modeling the nonlinear system. Also, an \mathcal{H}_∞ observer design with parameter-dependent stability is proposed to attenuate the disturbance impact on estimation error. Furthermore, the numerical simulation has proven the capability of the proposed observer design in attenuating the disturbance impact under the existence of Lipschitz nonlinearity. In the future, the impact of the time-delay problem on S-NLPV, as well as its observer design, will also be studied.

APPENDIX

SYSTEM REFORMULATION

Consider the following system with parameter-dependent output y :

$$\begin{cases} E\dot{x} &= A(\rho)x + B(\rho)u + B_{\phi(\rho)}\phi(x, u) + D_{1(\rho)}w \\ y &= C_{y(\rho)}x + D_{2(\rho)}w \\ z &= C_zx \end{cases} \quad (60)$$

To reformulate y into the parameter-independent output y^* , a stable filter F_y is proposed:

$$F_y: \begin{cases} x_F &= A_F x_F + C_F y, \\ y^* &= C_F x_F. \end{cases} \quad (61)$$

For example, this filter can be a low-pass filter whose cut-off frequency is high enough to not suppress the useful information/characteristic of output y . Thus, an augmented system, which has the same structure as (1), is obtained:

$$\begin{cases} \begin{bmatrix} E & 0 \\ 0 & I \end{bmatrix} \dot{x}_a &= \begin{bmatrix} A(\rho) & 0 \\ B_F C_{y(\rho)} & A_F \end{bmatrix} x_a + \begin{bmatrix} B(\rho) \\ 0 \end{bmatrix} u \\ &+ \begin{bmatrix} B_{\phi(\rho)} \\ 0 \end{bmatrix} \phi(Kx_a, u) + \begin{bmatrix} D_{1(\rho)} \\ B_F D_{2(\rho)} \end{bmatrix} w, \\ y^* &= \begin{bmatrix} 0 & C_F \end{bmatrix} x_a, \\ z &= \begin{bmatrix} C_z & 0 \end{bmatrix} x_a, \end{cases}$$

where $x_a = [x^T \ x_F^T]^T$; $K = [I_{n_x} \ 0]$; and γK is the new Lipschitz constant as $\|\phi(x, u) - \phi(\hat{x}, u)\| \leq \gamma K \|x_a - \hat{x}_a\|$ with \hat{x}_a is the estimated of x_a in observer design. Therefore,

without loss of generality, only the S-NLPV system (1) is studied.

REFERENCES

- [1] O. Sename, P. Gaspar, and J. Bokor, *Robust control and linear parameter varying approaches: Application to vehicle dynamics*. Berlin, Germany: Springer-Verlag, 2013.
- [2] L. Dai, *Singular control systems*. Springer, 1989, vol. 118.
- [3] H. Hamdi, M. Rodrigues, C. Mechmeche, D. Theilliol, and N. B. Braïek, "Fault detection and isolation in linear parameter-varying descriptor systems via proportional integral observer," *International journal of adaptive control and signal processing*, vol. 26, no. 3, pp. 224–240, 2012.
- [4] F. Shi and R. J. Patton, "Fault estimation and active fault tolerant control for linear parameter varying descriptor systems," *International Journal of Robust and Nonlinear Control*, vol. 25, no. 5, pp. 689–706, 2015.
- [5] M. Rodrigues, H. Hamdi, N. B. Braïek, and D. Theilliol, "Observer-based fault tolerant control design for a class of LPV descriptor systems," *Journal of the Franklin Institute*, vol. 351, no. 6, pp. 3104–3125, 2014.
- [6] F.-R. López-Estrada, J.-C. Ponsart, C.-M. Astorga-Zaragoza, J.-L. Camas-Anzueto, and D. Theilliol, "Robust sensor fault estimation for descriptor-LPV systems with unmeasurable gain scheduling functions: Application to an anaerobic bioreactor," *International Journal of Applied Mathematics and Computer Science*, vol. 25, no. 2, pp. 233–244, 2015.
- [7] B. Boukroune, A. Aitouche, and V. Cocquempot, "Observer design for nonlinear parameter-varying systems: Application to diesel engines," *International Journal of Adaptive Control and Signal Processing*, vol. 29, no. 2, pp. 143–157, 2015.
- [8] N. us Saqib, M. Rehan, N. Iqbal, and K.-S. Hong, "Static antiwindup design for nonlinear parameter varying systems with application to dc motor speed control under nonlinearities and load variations," *IEEE Transactions on Control Systems Technology*, vol. 26, no. 3, pp. 1091–1098, 2017.
- [9] R. Yang, D. Rotondo, and V. Puig, "D-stable controller design for lipschitz NLPVsystem," *IFAC-PapersOnLine*, vol. 52, no. 28, pp. 88–93, 2019.
- [10] T.-P. Pham, O. Sename, and L. Dugard, "Real-time damper force estimation of vehicle electrorheological suspension: A nonlinear parameter varying approach," *IFAC-PapersOnLine*, vol. 52, no. 28, pp. 94–99, 2019.
- [11] F. Wu, X. H. Yang, A. Packard, and G. Becker, "Induced \mathcal{L}_2 -norm control for LPV systems with bounded parameter variation rates," *International Journal of Robust and Nonlinear Control*, vol. 6, no. 9-10, pp. 983–998, 1996.
- [12] P. Apkarian, P. Gahinet, and G. Becker, "Self-scheduled \mathcal{H}_∞ control of linear parameter-varying systems: a design example," *Automatica*, vol. 31, no. 9, pp. 1251–1261, 1995.
- [13] S. Boyd, L. El Ghaoui, E. Feron, and V. Balakrishnan, *Linear matrix inequalities in system and control theory*. SIAM, 1994.
- [14] C. Hoffmann and H. Werner, "A survey of linear parameter-varying control applications validated by experiments or high-fidelity simulations," *IEEE Transactions on Control Systems Technology*, vol. 23, no. 2, pp. 416–433, 2015.
- [15] F. Wu, *Control of linear parameter varying systems (Ph.D. thesis)*. University of California, Berkeley, 1995.
- [16] P. Apkarian and R. J. Adams, "Advanced gain-scheduling techniques for uncertain systems," in *Advances in linear matrix inequality methods in control*. SIAM, 2000, pp. 209–228.
- [17] H. S. Abbas, A. Ali, S. M. Hashemi, and H. Werner, "LPV state-feedback control of a control moment gyroscope," *Control Engineering Practice*, vol. 24, pp. 129–137, 2014.
- [18] J. Lofberg, "Yalmip: A toolbox for modeling and optimization in matlab," in *Computer Aided Control Systems Design, 2004 IEEE International Symposium on*. IEEE, 2004, pp. 284–289.
- [19] K.-C. Toh, M. J. Todd, and R. H. Tütüncü, "Sdpt3 – a matlab software package for semidefinite programming, version 1.3," *Optimization methods and software*, vol. 11, no. 1-4, pp. 545–581, 1999.
- [20] D. Koenig and S. Mammam, "Design of proportional-integral observer for unknown input descriptor systems," *IEEE Transactions on Automatic Control*, vol. 47, no. 12, pp. 2057–2062, 2002.